

## Correlation-Driven Charge Order at the Interface between a Mott and a Band Insulator

Rossitza Pentcheva<sup>1,\*</sup> and Warren E. Pickett<sup>2</sup>

<sup>1</sup>Department of Earth and Environmental Sciences, University of Munich, Theresienstrasse 41, 80333 Munich, Germany

<sup>2</sup>Department of Physics, University of California, Davis, California 95616, USA

(Received 9 August 2006; published 5 July 2007)

To study digital Mott insulator  $\text{LaTiO}_3$  and band insulator  $\text{SrTiO}_3$  interfaces, we apply correlated band theory within the local density approximation including a Hubbard  $U$  to  $(n, m)$  multilayers,  $1 \leq n, m \leq 9$  using unit cells with larger lateral periodicity. If the on-site repulsion on Ti is big enough to model the Mott insulating behavior of undistorted  $\text{LaTiO}_3$ , the charge imbalance at the interface is found in all cases to be accommodated by disproportionation ( $\text{Ti}^{4+} + \text{Ti}^{3+}$ ), charge ordering, and  $\text{Ti}^{3+}$   $d_{xy}$ -orbital ordering, with antiferromagnetic exchange coupling between the spins in the interface layer. Lattice relaxations lead to conducting behavior by shifting (slightly but importantly) the lower Hubbard band, but the charge and orbital order is robust against relaxation.

DOI: [10.1103/PhysRevLett.99.016802](https://doi.org/10.1103/PhysRevLett.99.016802)

PACS numbers: 73.20.Hb, 71.28.+d, 75.70.Cn

Atomically abrupt (“digital”) interfaces (IFs) between oxides with strongly differing electronic properties (superconducting-ferromagnetic; ferroelectric-ferromagnetic) have attracted interest [1,2] due to the new behavior that may arise and for future device applications. Hwang and collaborators [3,4] grew coherent superlattices (SLs) containing a controllable number of layers of Mott insulator [ $\text{LaTiO}_3$  (LTO)] and band insulator [ $\text{SrTiO}_3$  (STO)] using pulsed laser deposition. The most provocative result was that the IFs of these insulators showed metallic conductivity and high mobility. In LTO/STO SLs, the transition metal ions on the perovskite  $B$  sublattice are identical (Ti) and only the charge-controlling  $A$  sublattice cations (Sr, La) change across the IF (cf. Fig. 1). Thus at the interface charge neutrality is violated, leaving a  $\text{TiO}_2$  layer with local environment midway between that in LTO and STO. Electron energy loss spectra for Ti indicated a superposition of  $\text{Ti}^{3+}$  and  $\text{Ti}^{4+}$  ions in the IF region. The magnetic behavior implicit in the occurrence of  $\text{Ti}^{3+}$  ions at the interface coupled with the realization of a two-dimensional electron gas suggests not only potential spintronics applications but also a new platform for studying magnetic impurities in two dimensions. Still, the mechanism of charge accommodation, the origin of conductivity, and the role of lattice defects are not unambiguously clarified [5–9].

The theoretical understanding of the phenomena arising at these IF was initiated by single- and three-band Hubbard modeling with screened intersite Coulomb interaction. Both the Hartree-Fock approximation or dynamical mean field theory with a semiclassical treatment of correlation [10] result in a ferromagnetic (FM) metallic IF over a substantial parameter range. *Ab initio* studies reported so far have studied charge profiles or lattice relaxations [11,12] while neglecting correlation effects beyond the local density approximation that we address below. Recent LDA +  $U$  calculations studied the effect of lattice

relaxations providing additional input into the Hubbard modeling [13] of this system.

In this Letter we focus on the compensation mechanism of the local charge imbalance at the IF and its role in the emergence of charge, magnetic, and orbitally ordered states distinct from the bulk phases by using the material-specific insight into correlated behavior that can only be obtained from first principles methods. We have performed density-functional theory calculations [within the generalized gradient approximation (GGA) [14]] with the all electron full-potential linearized augmented plane wave method in the WIEN2K implementation [15] including a Hubbard-type on-site Coulomb repulsion (LDA/GGA +  $U$ ) [16]. Among other material-specific aspects, these cal-

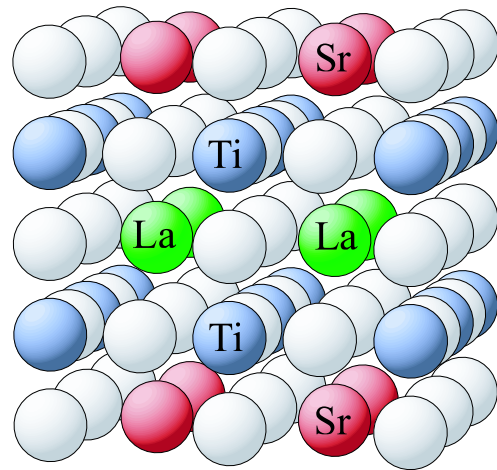


FIG. 1 (color online). Segment of the (1,1)  $\text{LaTiO}_3$ - $\text{SrTiO}_3$  multilayer, illustrating the cubic perovskite structure (unlabeled white spheres denote oxygen). An  $\text{LaO}$  layer lies in the center, bordered by two  $\text{TiO}_2$  layers, with a  $\text{SrO}$  layer at top and bottom. The lateral size of this figure corresponds to the  $p(2 \times 2)$  cell discussed in the text.

culations include electronic screening of the cations microscopically and self-consistently.

To explore the formation of possible charge disproportionated, magnetically ordered, and orbitally selective phases at the IF and to probe the relaxation length towards bulk behavior we have investigated a variety of  $(n, m)$  heterostructures with  $n$  LTO and  $m$  STO layers ( $1 \leq n, m \leq 9$ ). We have considered additional degrees of freedom that have not been addressed so far by using lateral cells of  $c(2 \times 2)$  or  $p(2 \times 2)$  [17]. The  $\hat{z}$  direction is taken perpendicular to the IF. Lattice parameters of the systems have been set to the experimental lattice constant of the STO substrate, 3.92 Å. Bulk STO is a band insulator with a GGA-band gap [14] of 2.0 eV (experimental value 3.2 eV), separating filled O  $2p$  bands from empty Ti  $3d$  bands.

Currently LTO ( $a = 3.97$  Å) and other  $3d^1$  perovskites are intensively studied because of their complex electronic and magnetic behavior [18]. Bulk LTO is an antiferromagnetic insulator of  $G$  type (rocksalt spin arrangement) with a gadolinium orthoferrite (20 atom) structure. However, x-ray diffraction studies on epitaxial LTO films grown on an STO substrate indicate a tetragonal instead of the bulk orthorhombic distortion [19]. Therefore, we first discuss results obtained for a cubic structure and then address the effect of tetragonal distortion. Using the LDA +  $U$  method, an insulator is obtained for  $U = 8$  eV and  $J = 1$  eV, consistent with electron-electron interaction parameters obtained from constrained local density approximation [20]. The magnetic moment  $M_{Ti} \approx 0.75\mu_B$  results from occupation of one of the  $t_{2g}$  orbitals (orbital ordering arising from spontaneous symmetry breaking). FM alignment of spins is 50 meV/Ti less favorable.

We discuss first the (1,1) multilayer pictured in Fig. 1, and then consider systems with thicker LTO and/or STO slabs to analyze the relaxation towards bulk behavior. The (1,1)-SL is modeled in a transverse  $c(2 \times 2)$  cell with two inequivalent Ti ions, which allows disproportionation within a single Ti layer and is consistent with the  $G$  type order in bulk LTO. The on-site repulsion strength  $U$  on Ti was varied from 0 to 8 eV to assess both weak and strong interaction limits. The Ti moment and the evolution of the density of states as a function of  $U$  are shown in Fig. 2(a) and 2(b), respectively. Within GGA ( $U = 0$ ) nonmagnetic metallic character is obtained, in line with earlier reports [11,12]. For  $U \leq 5$  eV the system is a FM metal with equivalent Ti ions (the magnetic moment saturates at  $0.33\mu_B$ ). This regime is qualitatively like earlier results on multiband Hubbard models [10]. At  $U \approx 5.5$  eV disproportionation occurs on the Ti sublattice, apparently weakly first-order as has been found in  $\text{Na}_x\text{CoO}_2$  [21]. Around  $U \approx 6$  eV there is a narrow half-metallic FM region, but beyond  $U \approx 6.5$  eV a gap opens separating the lower Hubbard band (LHB) and resulting in a correlated insulator phase. In the following we model the Mott insulating gap (0.5 eV) with  $U = 8$  eV and  $J = 1$  eV.

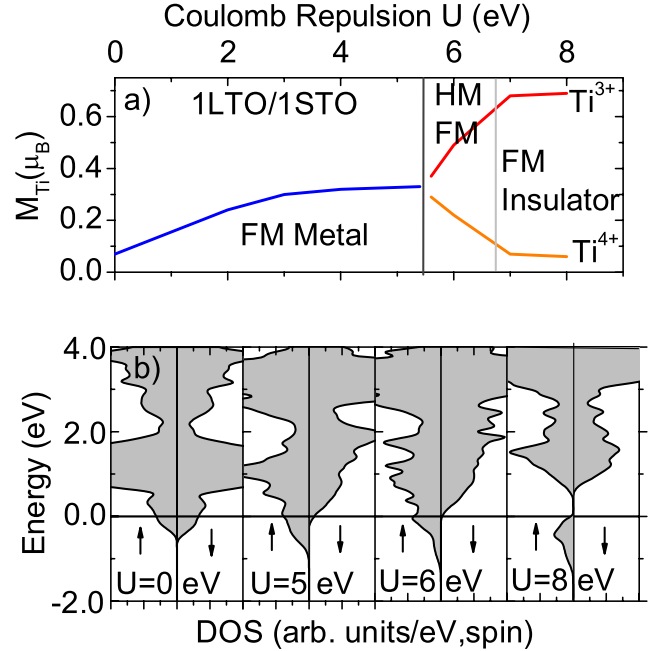


FIG. 2 (color online). (a) Phase diagram of the Ti moments for the (1,1)-SL in a transverse  $c(2 \times 2)$  cell vs the on-site Coulomb repulsion strength  $U$  on the Ti  $3d$  orbitals. (b) Density of states (spin direction indicated by arrows) of the (1,1)-SL for different  $U$  values. Disproportionation occurs in a weak first-order manner around  $U \approx 5.5$  eV. HM FM indicates a region of half-metallic ferromagnetism before the Mott gap appears around  $U \approx 6.5$  eV.

The arrangement of  $\text{Ti}^{3+}$ ,  $\text{Ti}^{4+}$  ions is charge-ordered (CO) rocksalt and retains inversion symmetry with the more highly charged  $d^0$  ions avoiding being nearest neighbors. The spatial distribution of the occupied  $d$  orbitals in the IF  $\text{TiO}_2$  layer displayed in Fig. 3 reveals that besides the CO this state is orbitally ordered (OO) with a filled  $d_{xy}$  orbital at the  $\text{Ti}^{3+}$  sites. Correlation together with the intrinsic symmetry-lowering effect of the IF lifts the three-fold degeneracy of the  $t_{2g}$  orbitals. The Fermi level lies in a small Mott gap separating the occupied narrow  $d_{xy}$  band (LHB) from the rest of the unoccupied  $d$  orbitals. For ferromagnetic alignment of the spins ( $M_{\text{Ti}^{3+}} = 0.72\mu_B$ ) the gap ensures an integer moment ( $2.0\mu_B$ ). We have also investigated an alignment of the spins by extending the calculation to a larger  $p(2 \times 2)$  cell and find the latter is preferred by 80 meV per  $p(2 \times 2)$  cell for the (1,1) superlattice (a spin-spin exchange coupling of  $|\mathcal{J}| = 10$  meV).

At the basic level of single band modeling this interface resembles the quarter-filled extended Hubbard model, which is known to be metallic even in the strong interaction regime. However, intersite repulsion (which is included self-consistently in our calculations) drives commensurate charge order in the extended Hubbard model [22,23]. For the IF addressed here this behavior arises entirely within the  $d_{xy}$  subsystem (similarly to the extended Hubbard model) and with accompanying magnetic order.

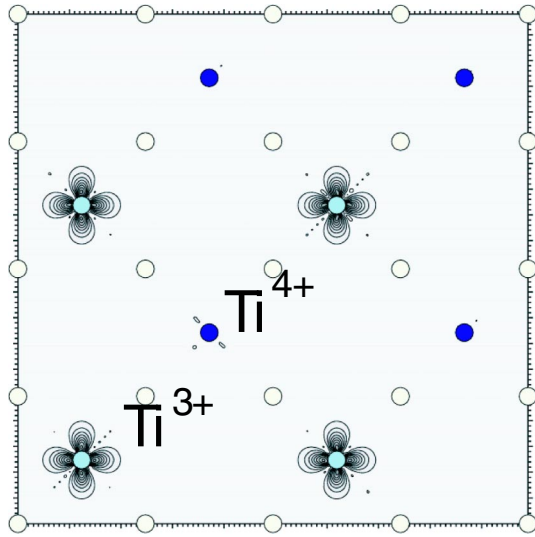


FIG. 3 (color online).  $45^\circ$  checkerboard charge density distribution of the occupied  $3d$  states in the charge-ordered  $\text{TiO}_2$  layer in the FM (1,1) multilayer. Orbital ordering due to  $d_{xy}$  orbital occupation is apparent. The positions of O,  $\text{Ti}^{3+}$ , and  $\text{Ti}^{4+}$  ions are marked by white, light blue (gray), and dark blue (black) circles, respectively.

*The (n, m)-SLs.*—To observe charge accommodation at more isolated IFs and examine relaxation towards bulk behavior, we have studied several thicker slabs containing  $(n, m)$  layers of LTO and STO, respectively, with  $1 \leq n, m \leq 9$ , all of which we find to be disproportionated, CO and OO, and insulating in the strong interaction regime. Following the experiment of Ohtomo *et al.* [3] we present results specifically for the (1,5) and (5,1) as well as the (5,5) superlattices. As is clear both from the layer-resolved magnetic moments presented in Table I and the layer-resolved projected density of states (DOS) for the (1,5) superlattice in Fig. 4(a), the IF  $\text{TiO}_2$  layer, and only this layer, is CO/OO with  $\text{Ti}^{3+}$  and  $\text{Ti}^{4+}$  distributed in a checkerboard manner. At every second Ti site the  $t_{2g}$  states split according to the IF-imposed symmetry lowering, and the  $d_{xy}$  orbital becomes occupied. The  $t_{2g}$  states on the  $\text{Ti}^{4+}$  ions remain essentially degenerate. Ti ions in neigh-

TABLE I. Layer-resolved magnetic moments (in  $\mu_B$ ) of the Ti ions in  $(n, m)$ -SLs containing  $n$  LTO and  $m$  STO layers. (1,5)\* denotes a configuration where the interlayer distances were relaxed according to Ref. [13].

System ( $n, m$ )	LTO		IF	STO	
	IF-2	IF-1	IF	IF + 1	IF + 2
(1,1)	...	...	0.72/0.05	...	...
(1,5)	...	...	0.71/0.05	0.0/0.0	0.0/0.0
(1,5)*	...	...	0.50/0.08	0.0/0.0	0.0/0.0
(5,1)	0.73/ - 0.73	-0.73/0.73	0.70/0.05	...	...
(5,5)	0.73/ - 0.73	-0.73/0.73	0.70/0.06	0.0/0.0	0.0/0.0

boring or deeper layers in the STO part of the slab have the configuration  $3d^0$  and are nonmagnetic, while those on the LTO side of the slab have the configuration  $3d^1$  and are  $G$  type ordered. Thus the charge mismatch is localized at the interface layer, with bulk LTO and STO character quickly reemerging on neighboring layers in contrast to the 1 nm relaxation length estimated from the electron energy loss spectra data [3].

The systems discussed so far are structurally perfect with ideal positions of the atoms in the perovskite lattice. Recently, two density-functional theory studies using GGA [12] and the LDA + U approach [13] investigated structural relaxations in LTO/STO-SLs, finding that Ti ions at the IF are displaced by 0.15 Å with respect to the oxygen ions leading to a longer Ti-Ti distance through the LaO layer than through the SrO layer. This “ferroelectric”-like distortion decays quickly in deeper lying layers. Using the relaxations reported in Ref. [13], we repeated the calculations for the (1,5) heterostructure. The resulting layer-resolved projected DOS at the Ti ions is displayed in Fig. 4(b). The most prominent feature is that for the relaxed structure the  $d_{xy}$  band (LHB) is shifted up by 0.4 eV with respect to the Fermi level and thus is only partially ( $\sim 70\%$ ) occupied. The charge is distributed in the minority spin channel at the  $\text{Ti}^{3+}$  sites (hybridization with O 2p bands) reducing the magnetic moment from  $0.71\mu_B$  in the

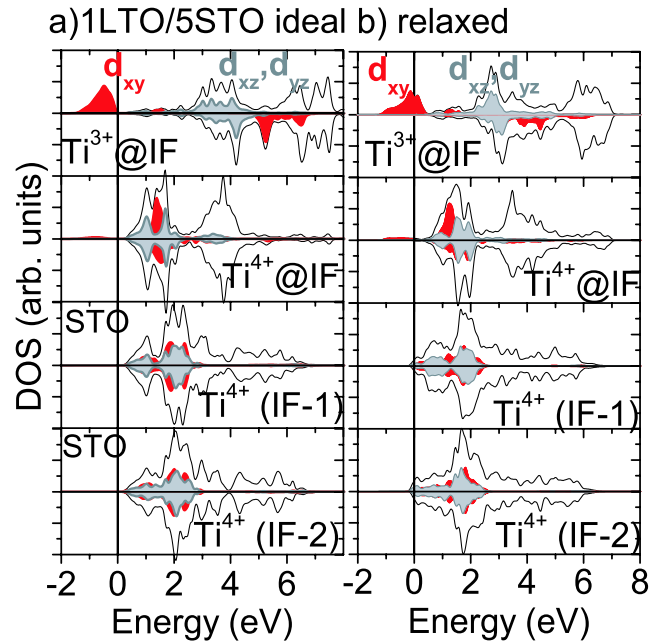


FIG. 4 (color online). Layer-resolved projected  $3d$  density of states at the Ti sites for a (a) structurally ideal and (b) relaxed (1,5) multilayer. The two topmost panels show  $\text{Ti}^{3+}$  and  $\text{Ti}^{4+}$  at the IF; the succeeding panels show the behavior of the Ti ion in deeper layers of the STO part of the slab. Ti  $d_{xy}$  orbitals are marked red (dark gray), while the  $d_{xz}$  and  $d_{yz}$  are marked light gray.

ideal structure to  $0.50\mu_B$ . Additionally there is a small contribution to conductivity of  $\text{Ti}^{4+}$  in deeper lying layers in the  $\text{SrTiO}_3$  host whose  $d$  bands now slightly overlap the Fermi level. Hence it is the lattice relaxations that result in a metallic heterostructure and a longer healing length towards bulk behavior, in agreement with the experimental observations [3,4] in spite of a majority of the charge being tied up at the IF. Still, the CO/OO arrangement remains; it is robust with respect to relaxation and tetragonal distortion. Recent resonant Ti  $2p$ - $3d$  photoemission spectra [24] of interfaces capped by one or two STO layers were interpreted by a dynamical mean field theory IF model without considering charge disproportionation. Although the LDA + U method is not a theory of excitation spectra, it is worth noticing that the spectral weight at and below the Fermi level obtained from photoemission spectra [24] is consistent in shape and width with the DOS in Fig. 4(b), arising from a localized electron on half of the Ti sites.

In summary, if the interaction strength  $U$  within the Ti  $3d$  states is large enough to reproduce the insulating state in cubic LTO, charge mismatch at  $\text{LaTiO}_3/\text{SrTiO}_3$  superlattices is found to be compensated within the IF layer itself by disproportionation, followed by charge order with  $\text{Ti}^{3+}$  and  $\text{Ti}^{4+}$  distributed in a checkerboard manner. Already the symmetry breaking at the interface (and not lattice relaxations) induces orbital-order in the IF layer, with an occupied  $d_{xy}$  orbital at the  $\text{Ti}^{3+}$  sites. This charge and orbital order emerging robustly in all systems studied is easily understood but unanticipated from the original reports on these heterostructures and could only be obtained by an explicit and self-consistent treatment of electronic correlation and additional degrees of freedom (larger lateral periodicity) not considered so far. Thus, in complex oxide heterostructures, charge disproportionation and CO offer an additional degree of freedom to compensate charge imbalance that is not available, e.g., in polar semiconductors. For the ideal structure, the CO/OO state is a very narrow gap insulator. Atomic relaxation at the IF shifts the  $\text{Ti}^{3+}$  lower Hubbard band upward leading to conducting behavior, which also implies a longer healing length towards bulk behavior, consistent with the experimental indications. The magnetic state at these IFs is also unexpected—while bulk  $\text{SrTiO}_3$  is nonmagnetic and  $\text{LaTiO}_3$  is an antiferromagnet, at these IFs we find a diluted layer of  $\text{Ti}^{3+}$  ion spins whose exchange coupling is antiferromagnetic in sign. Brinkman *et al.* recently found first experimental indications for localized magnetic moments in the related  $n$ -type  $\text{LaAlO}_3/\text{SrTiO}_3$  IF [25] supporting the picture predicted here and in Ref. [26].

We acknowledge discussions with J. Rustad and J. Kuneš and communication with A.J. Millis and N.A.

Spaldin. R. P. was supported through DOE Grant No. DE-FG02-04ER15498. W. E. P. was supported by DOE Grant No. DE-FG03-01ER45876 and the DOE Computational Materials Science Network. W. E. P. also acknowledges support from the Alexander von Humboldt Foundation and the hospitality of the MPI Stuttgart and IFW Dresden during the latter stages of this work.

\*pentcheva@lrz.uni-muenchen.de

- [1] I. Božović and J. N. Eckstein, *Solid State Phenomena* **61–62**, 9 (1998).
- [2] Y. Ijiri, *J. Phys. Condens. Matter* **14**, R947 (2002).
- [3] A. Ohtomo *et al.*, *Nature (London)* **419**, 378 (2002).
- [4] H. Y. Hwang, *MRS Bull.* **31**, 28 (2006).
- [5] H. Y. Hwang *et al.*, *Physica (Amsterdam)* **22E**, 712 (2004).
- [6] K. Shibuya *et al.*, *Jpn. J. Appl. Phys.* **43**, L1178 (2004).
- [7] D. A. Muller *et al.*, *Nature (London)* **430**, 657 (2004).
- [8] N. Nakagawa *et al.*, *Nat. Mater.* **5**, 204 (2006).
- [9] W. Siemons *et al.*, *Phys. Rev. Lett.* **98**, 196802 (2007).
- [10] S. Okamoto and A. J. Millis, *Nature (London)* **428**, 630 (2004); *Phys. Rev. B* **70**, 075101 (2004); **70**, 241104(R) (2004); *Phys. Rev. B* **72**, 235108 (2005).
- [11] Z. S. Popovic and S. Satpathy, *Phys. Rev. Lett.* **94**, 176805 (2005).
- [12] D. R. Hamann *et al.*, *Phys. Rev. B* **73**, 195403 (2006).
- [13] S. Okamoto, A. J. Millis, and N. A. Spaldin, *Phys. Rev. Lett.* **97**, 056802 (2006).
- [14] J. P. Perdew *et al.*, *Phys. Rev. Lett.* **77**, 3865 (1996).
- [15] P. Blaha *et al.*, *An Augmented Plane Wave + Local Orbitals Program for Calculating Crystal Properties* (Kalheinz Schwarz, Technical University of Wien, Vienna, 2001), ISBN 3-9501031-1-2.
- [16] V. I. Anisimov *et al.*, *Phys. Rev. B* **48**, 16929 (1993).
- [17] For the former cell 18  $k$  points in the irreducible part of the Brillouin zone were used. The sphere radii were, in bohr, 2.50 (La,Sr), 1.90 (Ti), 1.60 (O). Unoccupied La  $4f$  states may lie in the same energy range as the Ti  $3d$  states. Although both orbitals are quite localized and there is no hybridization between them, we have used  $U_{\text{La}} = 7.5$  eV to shift the empty  $f$  states to higher energies.
- [18] E. Pavarini *et al.*, *Phys. Rev. Lett.* **92**, 176403 (2004).
- [19] K. H. Kim *et al.*, *Phys. Status Solidi A* **200**, 346 (2003).
- [20] I. Solovyev *et al.*, *Phys. Rev. B* **53**, 7158 (1996).
- [21] K.-W. Lee *et al.*, *Phys. Rev. B* **70**, 045104 (2004); *Phys. Rev. Lett.* **94**, 026403 (2005).
- [22] S. Onari *et al.*, *Phys. Rev. B* **70**, 094523 (2004).
- [23] Y. Z. Zhang *et al.*, *Eur. Phys. J. B* **44**, 265 (2005).
- [24] M. Takizawa *et al.*, *Phys. Rev. Lett.* **97**, 057601 (2006).
- [25] A. Brinkman *et al.*, arXiv:cond-mat/0703028 [Nat. Mater. (to be published)].
- [26] R. Pentcheva and W. E. Pickett, *Phys. Rev. B* **74**, 035112 (2006).